Ultra-Robust Real-Time Estimation of Gait Phase

Mohammad Shushtari, Hannah Dinovitzer, Jiacheng Weng, and Arash Arami, *Member, IEEE*

***Abstract*— An ultra-robust accurate gait phase estimator is developed by training a time-delay neural network (D67) on data collected from the hip and knee joint angles of 14 participants during treadmill and overground walking. Collected data include normal gait at speeds ranging from 0.1m/s to 1.9m/s and conditions such as long stride, short stride, asymmetric walking, stop-start, and abrupt speed changes. Spatial analysis of our method indicates an average RMSE of 1.74±0.23% and 2.35±0.52% in gait phase estimation of test participants in the treadmill and overground walking, respectively. The temporal analysis reveals that D67 detects heel-strike events with an average MAE of 1.70±0.54% and 2.74±0.92% of step duration on test participants in the treadmill and overground walking, respectively. Both spatial and temporal performances are uniform across participants and gait conditions. Further analyses indicate the robustness of the D67 to smooth and abrupt speed changes, limping, variation of stride length, and sudden start or stop of walking. The performance of the D67 is also compared to the state-of-the-art techniques confirming the superior and comparable performance of the D67 to techniques without and with a ground contact sensor, respectively. The estimator is finally tested on a participant walking with an active exoskeleton, demonstrating the robustness of D67 in interaction with an exoskeleton without being trained on any data from the test subject with or without an exoskeleton.**

***Index Terms*— Gait phase, gait variability, pathological gait, rehabilitation, exoskeleton.**

I. Introduction

MOBILITY impairments are of the main challenges facing older adults as well as individuals suffering from stroke, or neurological conditions such as spinal cord injury, Parkinson's disease and multiple sclerosis. It is demonstrated that gait training in the early stages of recovery can help mitigate post-stroke motor deficits by forming new neural pathways [1], [2], [3]. Among the available solutions in this regard, lower limb exoskeletons offer high-intensity training sessions that can boost the neuromotor control recovery of affected individuals [4], [5]. In addition, these devices can prevent muscle atrophy, and improve the quality of life for people with motor deficits [6].

Control strategies are crucial to the efficacy of assistive devices [7]. Imposing a predefined trajectory using a trajectory controller can suppress the user's motor contributions which is shown to be disruptive to the motor rehabilitation of individuals who can still partially contribute to their motion [8]. A suitable strategy, therefore, must provide assistance as needed by guiding the motion while letting the user walk at a self-selected pace and pattern.

It is not easily possible to accomplish this goal with impedance control when a time-dependent reference trajectory is involved, since a trade-off has to be made between the spatial guidance and the temporal freedom [9]. Consequently, spatiotemporal decoupling is the key for an efficient assist-as-needed (AAN) control scheme, in which every leg needs its own reference trajectory independent of time. In this context, the gait phase is a suitable replacement for time [10], since it is monotonically increasing, reflecting gait events like heel-strike, and its derivative is proportional to the cadence.

Gait phase estimation has been widely used in control of assistive technologies such as lower-limb exoskeletons [11], [12], also in gait neuromechanical modeling and analysis such as joint impedance identification [13], [14] or estimation of gait spatiotemporal parameters [15].

Accurate real-time gait phase estimation is challenging, particularly, in case of pathological gait. Obtaining an accurate gait phase estimate is largely dependent on predicting the next gait event's timing. Typically, the gait phase is estimated as the ratio of the elapsed time from the latest heel-strike over the expected stride duration [16], [17]. As the estimated stride duration is updated at the end of each step, this method is only appropriate for conditions with low gait variability.

To address this issue, gait phase has been redefined and usually estimated according to joint angles or the body motion. In [18] and [19], for example, the phase-shift between the hip joint angle and its integral is interpreted as the gait phase. In [20], [21], [22], and [23], a cluster of adaptive oscillators (AO) is employed to lock to the hip angle phase and frequency or variation of leg's muscle shapes. Alternatively, a Kalman

Manuscript received 7 June 2022; revised 11 August 2022; accepted 12 September 2022. Date of publication 19 September 2022; date of current version 7 October 2022. This work is support in part by NSERC Discovery under Grant RGPIN-2018-04850, in part by John R. Evans Leaders Fund Canadian Foundation for Innovation, Ontario Research Fund (ORF), and in part by the New Frontiers in Research Fund under Grant NFRFE2018-01698. *(Corresponding author: Mohammad Shushtari.)*

This work involved human subjects or animals in its research. Approval of all ethical and experimental procedures and protocols was granted by the University of Waterloo Clinical Research Ethics Committee under Approval No. ORE#41794, and performed in line with the Declaration of Helsinki.

Mohammad Shushtari, Hannah Dinovitzer, and Jiacheng Weng are with the Department of Mechanical and Mechatronics Engineering, University of Waterloo, Waterloo, ON N2L 3G1, Canada (e-mail: smshushtari@uwaterloo.ca; hdinovitzer@uwaterloo.ca; jiacheng.weng@uwaterloo.ca).

Arash Arami is with the Department of Mechanical and Mechatronics Engineering, University of Waterloo, Waterloo, ON N2L 3G1, Canada, and also with the Toronto Rehabilitation Institute (KITE), University Health Network, Toronto, ON M5G 2A2, Canada (e-mail: arash.arami@uwaterloo.ca).

Digital Object Identifier 10.1109/TNSRE.2022.3207919

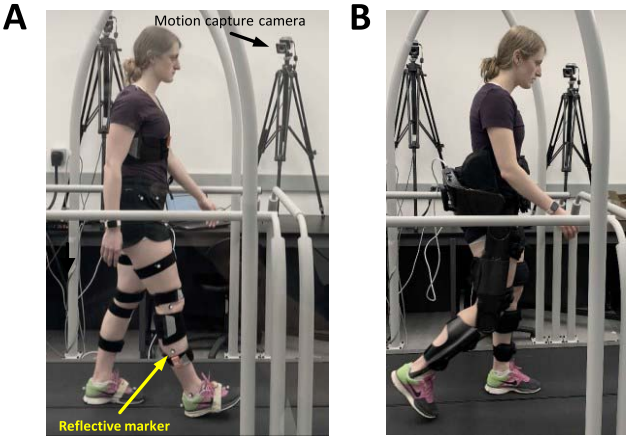

Fig. 1. Experimental setup: a participant walking on the treadmill **(A)** without and **(B)** with an exoskeleton. Participants kinematics are recorded using the motion capture and motor encoders during without and with exoskeleton walking, respectively. The ground reaction forces are collected by separate load cells under each belt of the treadmill. The participant has permitted usage of their photo in this paper.

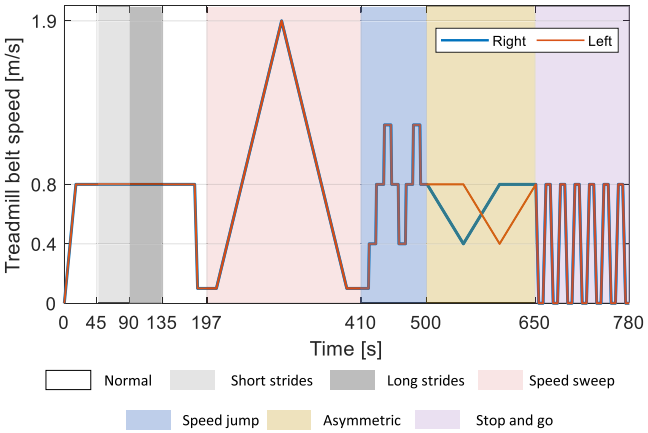

Fig. 2. The speed profile during the treadmill walking session. The right and left belts share the same speed profiles except during the asymmetric walking condition.

filter (KF) is used in [12] instead of AOs to estimate the gait phase. In these methods, gait speed changes are continuously reflected in the gait phase, however, with some lag due to the AO or the KF convergence dynamics. A solution is to reset the estimated gait phase to zero at each heel-strike, detected using a contact sensor. Such instantaneous correction of the gait phase error, leads to discontinuous estimation. The phase error is, therefore, gradually corrected to maintain the smoothness of the gait phase [21].

A more accurate gait phase estimation, nevertheless, requires more joints to be involved in the estimation process. As an example, the gait phase is estimated in [24] by finding a point on the hip-knee reference path that has the minimum distance from the current hip-knee coordinate. To include more kinematic features (e.g., joint velocity or body segments acceleration) data-driven models are widely used as they can learn the mapping from multi-dimensional kinematic space to the gait phase. A Robust estimator, on the other hand, is expected to provide an accurate mapping in a wide range of gait speeds, patterns, conditions, and user characteristics. Artificial Neural Networks (ANN) have the capability of learning such complex mapping.

In [25], for example, an ANN is used to estimate the gait phase at different speeds from the hip joint angle and trunk and thigh inertial measurement units (IMUs) data. Alternatively, long-short-term-memory (LSTM) networks are used to learn the gait phase from the IMU data [26], [27], [28]. Additionally, [29] uses a convolutional neural network (CNN) to estimate the gait phase while accounting for the variable gait patterns associated with stairways and ramps.

Using data-driven models, the problem of designing a robust and accurate gait phase estimator is turned into the problem of collecting a rich data set that enables the model to capture a generalizable yet accurate mapping between input data and the gait phase. The need for a specially designed and trained gait phase estimator is even more critical for gait training exoskeletons because they must be capable of assisting a broad spectrum of pathological gait patterns. The natural conflict in physical human-exoskeleton interaction also require extra robustness. Therefore, acceleration or velocity data, which have a higher sensitivity to emerging conflicts, have to be avoided as input features making the gait phase estimation even more difficult.

Currently, none of the existing studies are designed to provide accurate phase estimation during abnormal or pathological gait. They are also designed specific to a certain exoskeletons or prosthetic device. In this work, we present a real-time gait phase estimator that only uses the hip and knee angles as inputs and is specifically trained to maintain its performance on new participants without retraining and regardless of the assistive strategy, gait speed, gait pattern abnormalities such as asymmetry, during treadmill or overground walking. The proposed method is further compared to the state of the art techniques and tested as the core of an impedance controller implemented on an exoskeleton.

II. Methods and Material

A. Experimental Setup

Measurements of lower limb kinematics were carried out with a motion capture system that included eight Vero Cameras (Vicon, UK). The motion of the lower limbs was calibrated, labeled, and tracked using 16 reflective markers according to the Plug-In Gait convention [30]. An instrumented split-belt treadmill (Bertec, US), capable of measuring ground reaction forces (GRF) under each foot, was used to monitor and control the speed of each belt (Fig.1A). The treadmill and the motion capture data were synchronized and recorded at 1KHz and 100Hz, respectively. A lower limb exoskeleton (Indigo, Parker Hannifin, USA) with actuated hip and knee joints was also used, worn by an able-bodied individual, to test the performance of the gait phase estimator in the presence of an exoskeleton. The exoskeleton sensory data as well as control commands are transmitted at 200Hz.

B. Experimental Protocol

Fourteen participants (age: 28±4 years, body mass: 75.2±17.6 kg, height: 176.6±6.8 cm, 7 females and 7 males) with no known musculoskeletal impairments participated in

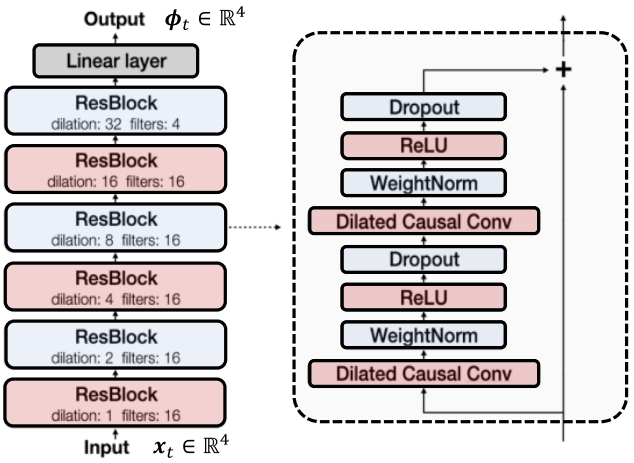

Fig. 3. The TCN network consists of six residual blocks, each including two dilated convolutional layers with the same dilation factor. Instantaneous joint angles (x_t) are fed into the first residual block while the output of the last residual block is fed into a linear layer to generate the final gait phase predictions (ϕ_t). The dropout rate is set to 0.1 for all residual blocks. Kernel size of 3 is used for all dilated causal convolutional layers.

this study. All participants provided informed consent prior to the experiment. The study protocol and procedures were approved by the University of Waterloo Clinical Research Ethics Committee (ORE#41794) and conformed with the Declaration of Helsinki.

The experiment involved treadmill and overground sessions. The treadmill session consisted of walking without the help of handrails in 8 different conditions for a total of 13 minutes (see Fig. 2). The first four conditions of the test consisted of walking at a constant speed of 0.8 m/s where the participants were asked to walk normally, with short strides, with long strides, and then again normally (for 45 seconds each). The fifth condition of the test included a speed sweep where the treadmill speed increased from 0.1m/s to 1.9m/s with a constant acceleration of 0.02m/s^2, immediately followed by a constant speed decrease back to 0.1m/s at the same rate. The sixth condition involved speed jumps between 0.4m/s, 0.8m/s, and 1.2m/s. The acceleration of the treadmill during these jumps was 0.4m/s^2. The seventh condition involved asymmetrical walking. Gait asymmetry was imposed by driving the treadmill belts with different speeds, up to a speed difference of 0.4m/s. As one of the most prominent asymmetric features observed in post-stroke patients, we used the swing time ratio ($t_{\text{longer}}/t_{\text{shorter}}$) for validation of the protocol [31], [32]. The speed difference between treadmill belts was chosen to have a maximum swing time ratio of 1.41±0.19 on average for all participants falling within the reported average values of 1.24 [32] and 1.44 [31]. The eighth and final condition involved repetitions of start walking, at a speed of 0.8m/s, and stop walking.

To check the sensitivity of the developed gait phase estimator to the exoskeleton dynamics and its controller effect, one participant repeated the same experiment two more times while wearing the exoskeleton; once in the Passive mode (controller was off) and once in the Active mode (controller was on). In the Active mode, the exoskeleton joints were controlled using the trained gait phase estimator embedded

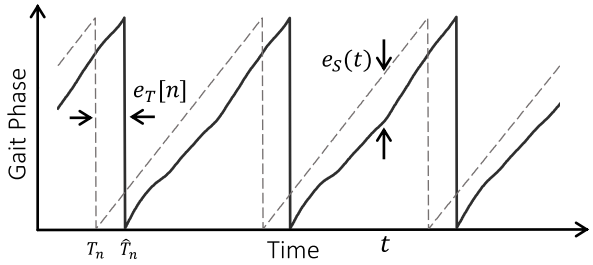

Fig. 4. Spatial (e_S) and Temporal (e_T) error according to the estimated and target gait phase profiles. The temporal error (e_T) is computed at the nth heel-strike event.

in a path controller [9] with the following joint stiffness (K) and damping (D) coefficients: $K_{\text{Hip}} = 300\ N.m.rad^{-1}$, $D_{\text{Hip}} = 45\ N.m.s.rad^{-1}$, $K_{\text{Knee}} = 65\ N.m.rad^{-1}$, $D_{\text{Knee}} = 25\ N.m.s.rad^{-1}$. The same impedance values were used for both legs. The reference path was taken from [10].

The overground session consisted of walking on a 10-meter straight path, three times with the following conditions: normal walking, slow walking, fast walking, short strides, and long strides. The participants were instructed to walk at a self-selected pace and adjust as they see fit for the trials at faster and slower speeds.

C. Training and Evaluation of the Gait Phase Estimator

Collected data, including joint angles, marker positions, and GRF were filtered using a Woltring filter [33]. A Boolean stance flag, $S(t)$, was then computed as

$$S(t) = \text{sgn}(\max(F_{GR}(t) - F_{th}, 0)) \quad (1)$$

where $F_{GR}(t) \geq 0$ is the vertical GRF and F_{th} is a threshold set to 0.01 of each participant's weight. The heel-strike event is then detected from the rising edge of the stance flag. The heel-strike events in overground walking, when GRF was not measured, was extracted by applying the Foot Velocity Algorithm (FVA) [34] on the foot marker data. The target gait phase ($\boldsymbol{y}$) is then determined according to [10] as a monotonically increasing line going from 0 to 1 between two consecutive heel-strikes. The target gait phase values are then transformed to an extended description as $\boldsymbol{\phi} = [\phi_1, \phi_2, \phi_3, \phi_4]^T = [\sin(2\pi\, y_R), \cos(2\pi\, y_R), \sin(2\pi\, y_L), \cos(2\pi\, y_L)]^T$ before being utilized in the training of gait phase estimator. Such transformation avoids the sharp gait phase transition in the 0 to 1 representation which is easier for a data-driven model, e.g., a neural network, to represent. A time-delay neural network [35] with 67 input delays (D67 network) was trained separately using the scaled conjugate gradient backpropagation algorithm [36] to learn the mapping from both legs' hip and knee joint angles (input: $\boldsymbol{x} = [\theta_{\text{Hip},R}, \theta_{\text{Knee},R}, \theta_{\text{Hip},L}, \theta_{\text{Knee},L}]^T$) to the extended target gait phase ($\boldsymbol{\phi}$) by minimizing a loss function of the mean square error (MSE) between the estimated and the target extended gait phase. We note that our model is not sensitive to the method by which the joint angles are computed as long as they are accurate enough. For example, motor encoders are later used instead of motion capture to measure joint angle in an exoskeleton-assisted walking scenario(Section III-B). The

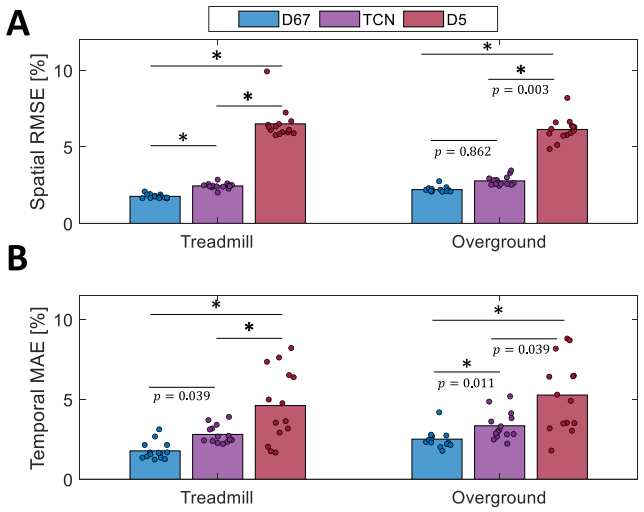

Fig. 5. (A) Spatial Accuracy comparison between the D67, TCN, and D5 networks. The circles in each pair of network and condition indicate the mean of spatial RMSE across all gait cycles of each participant in all conditions. The average spatial RMSE across the subjects is also represented with the respective bar height. Similarly, (B) compares the temporal MAE of the three networks in treadmill and overground walking conditions. The comparisons denoted by asterisks show significant difference between the average performance of the compared networks. The p-value is smaller than 0.001 unless specified.

D67 network consisted of three hidden layers of 30, 20, and 10 neurons with Relu activation functions. The input data to the network is $\boldsymbol{X} = [\boldsymbol{x}, \boldsymbol{x}_1, \ldots, \boldsymbol{x}_{67}]$ where $\boldsymbol{x}_n$ is the joint angles delayed by $d_n = \sum_{i=1}^{n} 1 + \lfloor 1.1^i/15 \rfloor$ samples where $\lfloor\ \rfloor$ is the floor operator. This way, the sampling density is decreased for older samples enabling the network to increase its memory horizon up to 473 samples (2.365s). For example, in a normal gait with 1.23s step time duration, the first 50 inputs of the network are sampled from the last half-step-time, while only 8 inputs are sampled with more than a step-time delay.

Besides the D67 network, we constructed two baseline networks. The first one is a Temporal Convolutional Network (TCN), i.e. a modern convolutional architecture capable of capturing long-term dependency of the input similar to recurrent networks while maintaining high computational efficiency of the convolutional operations [37]. Our TCN formulation and network hyper-parameters can be found in Fig. 3. Instantaneous joint angles ($\boldsymbol{x}(t)$) are used as an input to the TCN while the dilation factors are increased exponentially across the residual blocks to ensure wide receptive fields. The number of residual blocks is chosen such that the receptive field of the neurons in the last dilated causal convolutional layer covers roughly the period of one full gait cycle. The second baseline network is a time-delay neural network with two hidden layers of 5 neurons with 5 input delays (D5 network). Compared to the previous studies such as [29], [38] which have a 0.3s of sampling buffer, the D5 network has only a 0.025s of sampling buffer, serving as a model with minimum complexity to evaluate if employing more complex network architectures is worth the performance improvement.

We used leave-one-subject-out cross validation to test the neural networks' performance on each subject (training on 13 subjects' data, testing on one, and repeating the process for all fourteen subjects). Training was performed using treadmill and overground walking data of twelve subjects for updating the neural network weights, while training stop condition was checked using one randomly selected subject. Walking data with exoskeleton are not included in training or validation but are kept apart to evaluate the the estimated gait phase sensitivity to the possible effects of the exoskeleton dynamics and controller. The network estimate ($\hat{\boldsymbol{\phi}}$) is then transformed to the vector of left and right gait phases ($\hat{\boldsymbol{y}}$) using

$$\hat{\boldsymbol{y}} = 0.5 + \frac{1}{2\pi}[\text{atan2}(\hat{\phi}_1, \hat{\phi}_2), \text{atan2}(\hat{\phi}_3, \hat{\phi}_4)]^T. \quad (2)$$

The instantaneous spatial gait phase estimation error is defined as $\boldsymbol{e_S}(t) = \boldsymbol{y}(t) - \hat{\boldsymbol{y}}(\boldsymbol{t})$. The spatial root mean square error (RMSE) of gait phase estimation over each gait cycle is then computed to compare the spatial performance of the networks. The temporal error is also defined as $\boldsymbol{e_T}[n] = T_n - \hat{T}_n$ where T_n and $\hat{T}_n$ are the n^{th} heel-strike time detected from target and estimated gait phase, respectively. $\boldsymbol{e_T}[n]$ in then divided by the duration of n^{th} stride (separately for the left and the right legs) to normalize the temporal error across different conditions (e.g., long or short strides). Temporal mean absolute error (MAE) is used as a compact measure for between-network comparisons. The statistical differences are identified by applying a two-sample Kolmogrov-Smirinov test with a significance level set to 0.05 with a Bonferroni correction being applied when comparing the three networks.

TABLE I
COMPARISON OF D67, TCN, AND D5 NETWORK PERFORMANCES

Session	Network	Spatial RMSE [%]	Temporal MAE [%]
Treadmill Walking	D67	1.74 ± 0.23	1.70 ± 0.54
	TCN	2.57 ± 0.79	2.87 ± 0.55
	D5	6.41 ± 3.30	4.37 ± 2.27
Overground Walking	D67	2.35 ± 0.52	2.74 ± 0.92
	TCN	2.69 ± 1.40	3.65 ± 1.35
	D5	6.33 ± 3.47	5.26 ± 2.32

III. RESULTS AND DISCUSSION

The overall spatial and temporal performances of D67, TCN, and D5 networks on the test participants across all trials are compared in Fig 5 and Table I. The D67 network outperforms the TCN network with 32.3% and 39.3% smaller spatial and temporal errors during the treadmill session, respectively. The D67 also exhibits 24.9% smaller temporal MAE in overground walking. The spatial performance, however, is not significantly different between the D67 and the TCN networks during the overground session. D67 network significantly outperforms the D5 spatially and temporally in treadmill walking and spatially in overground walking. The similar observation applies to the TCN except for the temporal performance during the overground walking. In all cases, D67 and TCN have a more uniform spatial and temporal performance across all participants, confirming the generalization of the trained models. D5 performance, in contrast, has greater variations,

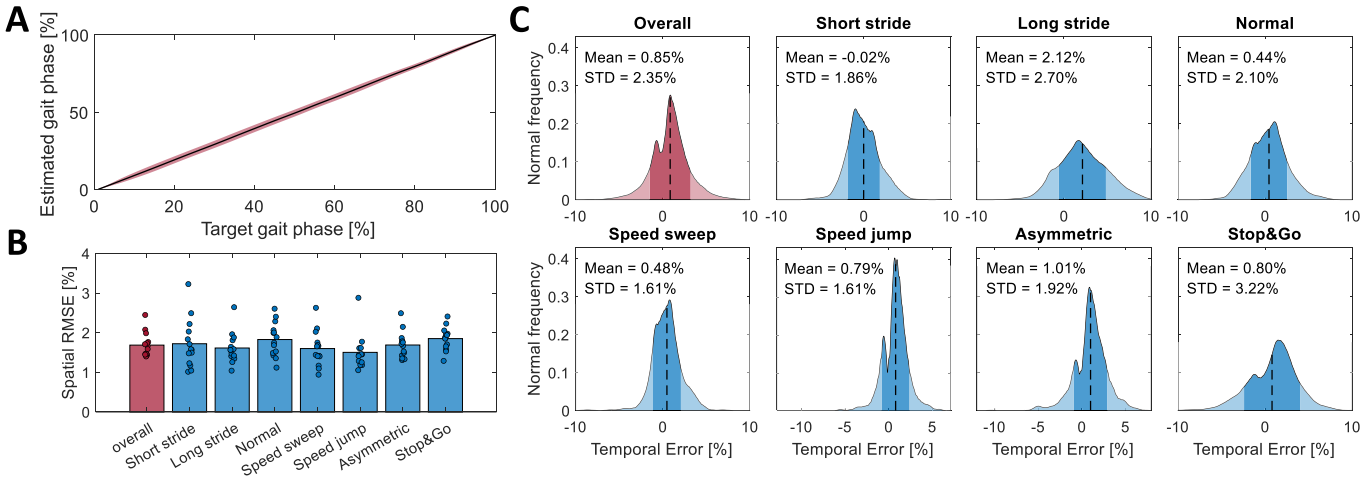

Fig. 6. The performance of the D67 network in treadmill walking gait phase estimation. (**A**) The average estimated gait phase profile with respect to the target gait phase. Gait phase estimation standard deviation is shaded in red. (**B**) The spatial RMSE of the estimated gait phase across the strides in each condition made by all participants. The average RMSE of gait phase estimation at each condition is represented by the respective bar height. (**C**) The estimated gait phase temporal error across all participants in each condition. The mean and standard deviation of the temporal error are depicted by dashed lines and bold areas, respectively.

particularly, in terms of temporal MAE implying the lack of expressivity in D5.

A. Detailed Performance Analysis

We now focus on D67 network for more detailed analysis of gait phase estimation performance across different conditions in both treadmill and overground walking.

1) Treadmill Walking: Fig.6.A shows the average estimated gait phase spatial profile with respect to the target gait phase across all gait cycles in different conditions in treadmill walking. The coefficient of determination for the estimated gait phase is greater than 0.999 that along with its negligible standard deviation confirm the accuracy and generalization of the D67 network.

The spatial performance across different experiment condition is further investigated in Fig.6.B where the mean Spatial RMSE is plotted for each participant along with the total mean Spatial RMSE across all participants in each condition. The standard deviation of mean performance across all conditions is 0.12%, indicating consistent generalization of the D67 model over experiment conditions.

Fig.6.C illustrates the distribution of the temporal error across experiment conditions. The D67 has accurately detected heel-strike events on average 0.85% earlier (e.g., about 10ms earlier in a stride with duration of 1.2s). The leading temporal estimation is, however, not consistent as the multimodal distribution of temporal error reveals that the estimated heel-strike event lags behind the actual event rather than leading for a sub-group of participants and conditions. The magnitude of the temporal error is, nevertheless, consistently small in treadmill and overground sessions across all experiment conditions showing the accuracy of D67 in heel-strike detection based on the hip and knee joint angles.

2) Overground Walking: The average estimated gait phase profile across all gait cycles in different conditions during overground walking is depicted in Fig.7.A showing a slight increase in standard deviation compared to the treadmill walking. Fig.7.B provides further details on the spatial performance for each participant across different conditions, indicating the D67 network's consistent performance.

In contrast to the treadmill session, the heel-strike detection takes place with a small but consistent lag during the overground walking. Fig.7.C illustrates that the heel-strike event is detected -1.83% later than the actual event (e.g., about 21ms later with a 1.2s stride time). This implies that the controlled condition in treadmill walking enables the model to better capture the gait dynamics and therefore, predict the heel-strike accurately. Moreover, the heel-strike events are reflected in the target gait phase with higher precision during treadmill walking than the overground walking due to the higher accuracy of force-based heel-strike detection than the marker-based method. Henceforth, the D67 network has probably learnt the heel-strike timings more precisely in treadmill walking.

B. Gait Phase Estimation in Presence of an Exoskeleton

In contrast to the previous tests, we used the joint angles computed by the exoskeleton motor encoders as the gait phase estimator inputs. The spatial performance of the D67 in presence of the exoskeleton in the Passive mode and Active mode in treadmill walking is shown in Fig.8.A,B, respectively. The D67 exhibits a slightly smaller spatial error ($1.67\pm0.67\%$) compared to the treadmill session without the exoskeleton. The exoskeleton regularizes gait in the Passive mode due to its passive dynamics (i.e., inertia and friction) which causes the human lower limb motion to be damped and, therefore, restricts the kinematic variability. In the Active mode, in contrast, the spatial error increases by almost 100% and reaches to $3.49\pm1.06\%$ which is still sufficiently accurate for the exoskeleton controller to provide assistance properly in all experiment conditions. The decrease in the gait phase estimation performance stems from the human-exoskeleton

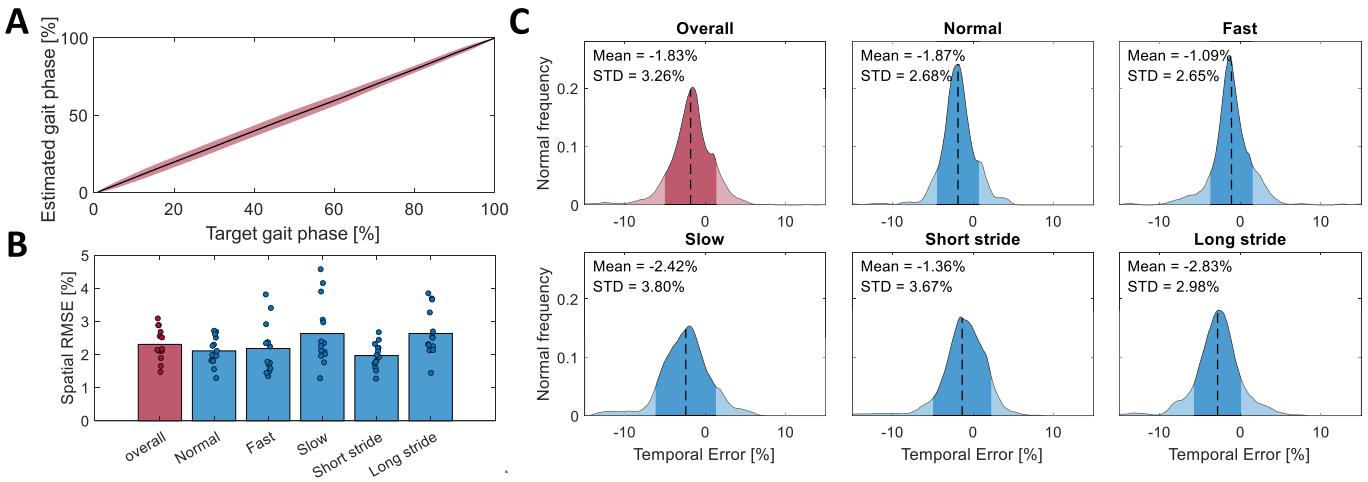

Fig. 7. The performance of the D67 network in overground walking gait phase estimation. Figure description is the same as Fig. 6

occasional conflicts in leading the motion since the exoskeleton assistance was not always aligned with the user intention. These conflicts emerge as excessive interaction force which to some extent distorts the gait pattern and, therefore, worsen the gait phase estimation performance. The overall estimated gait phase profile is illustrated in Fig. 8.A. A slight distortion is noticeable in the overall gait phase both in the Passive and Active modes compared to treadmill walking without exoskeleton. This is because of the exoskeleton effect on gait pattern. The gait phase profile in the Active mode also demonstrates a higher standard deviation due to the human-exoskeleton conflicts. Furthermore, the temporal error distribution in Fig.8.C exhibits greater standard deviation in the Active exoskeleton mode compared to the Passive mode and no exoskeleton conditions. The Spatial distortion and the higher temporal error standard deviation issues in the Active exoskeleton mode could be alleviated by incorporating the data from walking in presence of exoskeleton in the training. This is, however, not suggested as it reduces the generalizability and robustness of the model to different exoskeleton structures and controller designs (e.g., reference trajectory and controller impedance).

C. Robustness Analysis

To compare the robustness of the trained gait phase estimators, we scrutinized the gait phase estimation in the *speed jump*, *asymmetric gait*, and *stop and go* conditions.

1) Abrupt Speed Change: We considered a single stride in the speed jump condition where the treadmill speed abruptly changes from 0.8m/s to 1.2m/s. Fig.9.A shows the estimated gait phase profiles averaged over all participants. While D67 and TCN network demonstrate a negligible standard deviation, the D5 exhibits an unstable gait phase estimation facing the sudden change of the treadmill speed which has led to a standard deviation more than 20%. This analysis reveals that D5 network is of no use in daily life where an exoskeleton user frequently decides to switch their gait speed. According to the overall results represented in Fig.5, however, the D5 network seems to have an acceptable performance. It even seems to be a better option for a practical purpose where lower computational complexity and simple implementation is an advantage. Nevertheless, the recent robustness analysis shows that the overall performance measures such as RMSE, which is widely used in the literature, are not sufficient for validating the performance of a gait phase estimator.

Robustness of D67 network is further investigated in strides when the treadmill speed has jumped back and forth between 0.4m/s, 0.8m/s, and 1.2m/s in Fig.9.B. The estimated gait phase remained smooth for all of the participants in all cases. The highest gait phase variation is observed in case of 0.4m/s to 0.8m/s speed increase. In general, the gait phase estimation is more variable in the case of abrupt increase in the speed rather than abrupt decrease.

2) Asymmetric Gait: Fig.(10) shows the performance of D67 in asymmetric gait condition. The spatial and temporal errors are always less than 4.81% and 6.16%, respectively, indicating stability and robustness of the estimation. As the speed difference between treadmill belts increases, the spatial error in the phase estimation of both legs increases. This is however, more stressed for the left leg during the right leg limping interval. The opposite is also valid during the left leg limping interval.

3) Stop and Start: Fig.(11) Shows the estimated gait phase of participant #5 with and without exoskeleton as the treadmill stops and start running again. The estimated gait phase during walking without exoskeleton and with the exoskeleton in Passive mode smoothly converges to a constant level when the treadmill stops and maintains that level until the treadmill starts running again. In the Active exoskeleton mode, the estimated gait phase slope decreases gradually as the treadmill stops. During the stop interval, however, the estimator exhibits some oscillations on the gait phase which are due to the controller design rather than the sensitivity of the gait phase estimator. With a fixed gait phase in the stop interval, the exoskeleton imposes a fixed posture and therefore, fights against the natural human motions (such as shifting the body load between legs). The resultant conflict, as mentioned earlier, disturbs the estimated gait phase.

D. Comparison With the State of the Art

The performance of the D67 network is further compared to the performance of other gait phase estimators reported

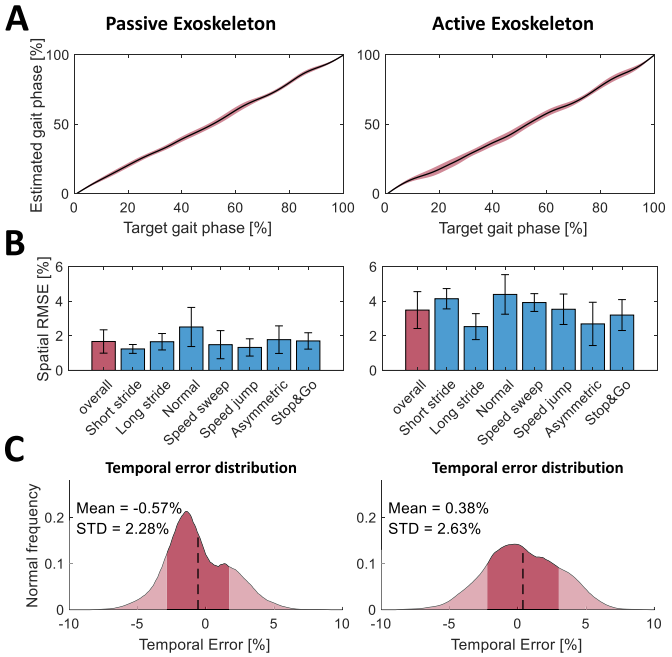

Fig. 8. The comparison between the temporal and spatial performance of the D67 network in treadmill walking with the Passive and Active exoskeleton on participant #5. **(A)** Overall average gait phase profiles in Passive and Active modes across experiment conditions. The shaded area shows the standard deviation. **(B)** The spatial performance across the experiment conditions in the Active and Passive control modes. **(C)** The temporal error distribution across all conditions in case of the Passive and Active exoskeletons. The mean and standard deviation of temporal errors are denoted by dashed lines and dark shaded area under the curves, respectively.

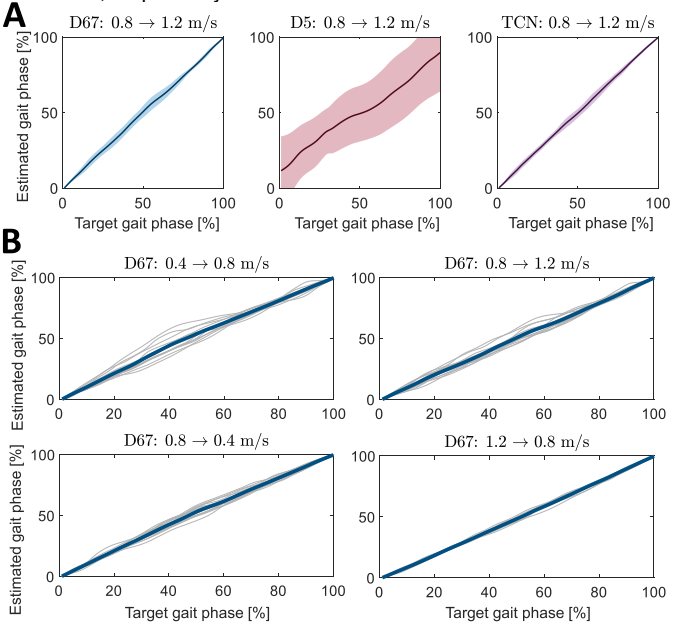

Fig. 9. **(A)** Comparison of D67, D5, and TCN networks estimated gait phase mean and standard deviation (denoted by shaded area) as the treadmill speed jumped from 0.8 to 1.2m/s averaged across all participants. **(B)** Detailed performance of the D67 network gait phase estimation in different speed jump scenarios. Each gray line represents one of the subjects while the blue line shows the average gait phase profile.

in literature for constant speed walking, speed jumps, and speed sweep on treadmill walking as well as overground walking at self-selected speed. We used three time-based gait phase estimators (TBEs) developed by Lenzi *et al.* [16],

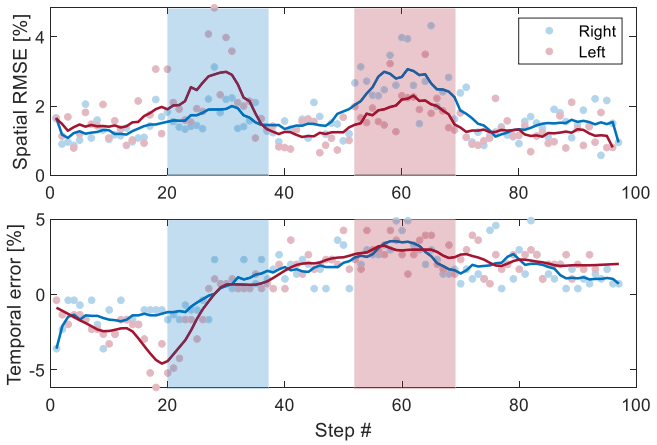

Fig. 10. D67 spatial and temporal performance for each step of the right and left legs during asymmetric walking. The blue and red circles show the performance at each step while the corresponding curve show the smoothed performance. The intervals during which the right and left legs are severely limping are denoted by blue and red shaded areas, respectively.

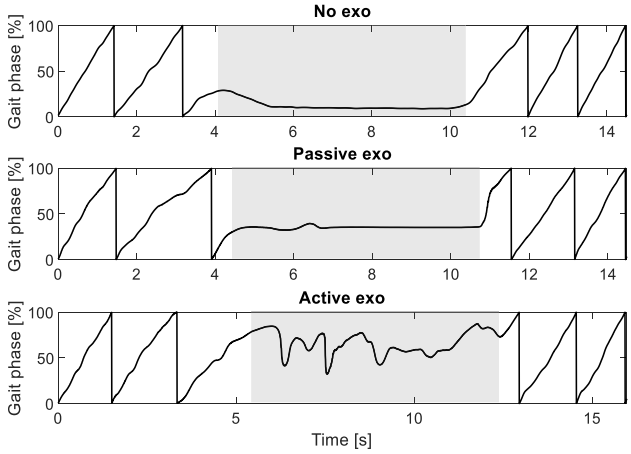

Fig. 11. D67 gait phase estimates when the treadmill belts have stopped and start moving again for participant #5 without exoskeleton and with the exoskeleton in the Passive and Active mode, respectively. The shaded area shows the interval when the treadmill belts were fully stopped.

Ferris *et al.* [17], and Kang *et al.* [25] as baselines along with the following methods compared to the D67

- **Kang(NN):** A neural network (reffered to as the independent model) trained for gait phase estimation on new participant similar to D67. The model is trained on a range of speeds between 0.6 and 1m/s, which includes steady state walking at 0.8m/s as well as speed jumps with accelerations of 0.05m/s^2.
- **Kang(CNN):** Later in [29], Kang et at. trained a CNN for gait phase estimation for level ground and ramp walking as well as stair ascend and descend.
- **Yan(AO):** An AO-based gait phase estimator developed by Yan *et al.* in [21] that uses foot contact sensors for phase error correction. D67 is compared to the vGRF variation of their method as it has the similar definition for gait phase. Yan(AO), Lenzi(TBE), and Ferris(TBE) methods are tested in this work during steady state walking at 0.67, 0.94, and 1.22m/s. They are additionally

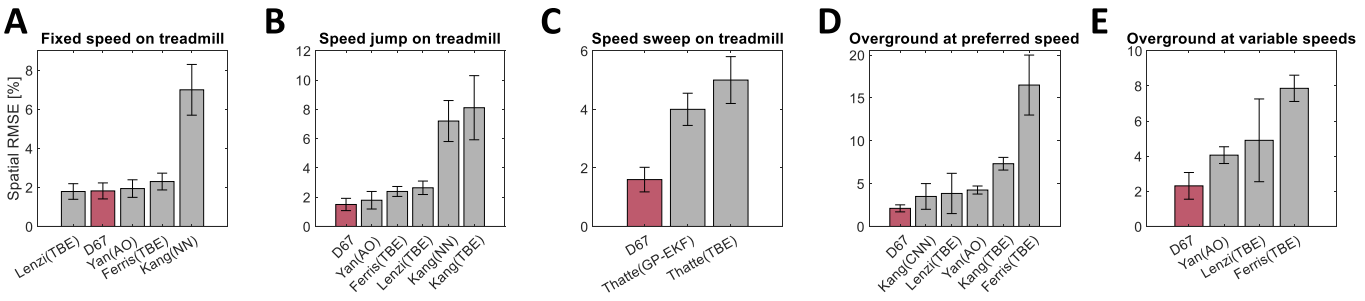

Fig. 12. Comparison of D67 gait phase estimator performance with approaches reported in the literature for (A) fixed speed, (B) speed jumps, and (C) speed sweep in treadmill walking as well as overground walking at (D) preferred speed and (E) variable speeds.

tested during speed jumps between the aforementioned speeds with an acceleration of 0.028m/s^2.

- **Thatte(GP-EKF):** A gait phase estimator developed by Thatte *et al.* [12] using Gaussian Process extended Kalman filter (GP-EKF). This method is tested on treadmill walking with a sinusoidal speed profile varying between 0.4 and 1.2m/s with a 20s period.

In fixed speed treadmill walking (Fig.12.A) the D67 has an RMSE of 1.82±0.41% for steady state walking at 0.8m/s outperforming all the competents but the Lenzi(TBE) which has a slightly better performance. The well-controlled gait conditions during fixed-speed treadmill walking causes lower variation in step duration and gait pattern allowing TB methods to provide accurate estimations. Besides Kang(NN), other methods also rely on heel-strike detection sensors. D67, in contrast, uses only joint angles and still provides the second best accuracy.

Fig.12.B shows the comparison in speed jump condition on treadmill. Kang(NN) and Kang(TBE) is tested on speed jumps between 0.6 and 1m/s with an unreported acceleration. The D67 network, with an RMSE of 1.5±0.42%, outperforms all approaches despite not using any contact sensors.

The comparison in speed sweep condition is illustrated in Fig.12.C. The D67 network resulted in RMSE of 1.6±0.42% while the Thatte (GP-EKF) method obtained 4±0.55% RMSE during the speed sweep experiment. For a more realistic comparison, however, both approaches should be tested on the same condition.

There is no comparable gait phase estimator presented in the literature with reported performance on asymmetric gait. As a close study, however, we also compared our method's performance with Thatte (GP-EKF) for walking with one prosthetic leg. As the other leg is intact in that study, some asymmetric features are presented in the gait. Our method resulted in RMSE of 1.69±0.33% and Thatte (GP-EKF) resulted in RMSE of 4±0.55% RMSE. For a more realistic comparison, however, both approaches should be tested under the same conditions.

With an RMSE of 2.11±0.41%, the D67 outperforms the Kang(CNN) with a RMSE of 3.5±1.5%, the YAN(AO) with performance of 4.25±0.47%, and the rest of the time-based methods in overground walking with preferred speed (see Fig.12.D). The D67 maintains its edge over the YAN(AO) and the time-based methods in overground walking with variable speed with an average RMSE of 2.31±0.76% as illustrated in Fig.12.E.

IV. Conclusion

In this study, a time-delay neural network (D67) is trained using hip and knee joint angles collected from 14 participants walking on a treadmill and overground to develop an accurate and robust gait phase estimator. Several types of gait data were collected in the study including normal gait at speeds between 0.1m/s and 1.9m/s and conditions such as long stride, short stride, asymmetric walking, stop-start, and abrupt speed changes. On average, our model's RMSE for gait phase estimation on treadmill walking and overground walking was 1.74±0.23%, and 2.35±0.52%, respectively. The temporal analysis also revealed that D67 was able to detect heel-strike events with an average MAE of 1.70±0.54% and 2.74±0.92% for treadmill and overground walking, respectively. Across participants and gait conditions, spatial and temporal performance is found to be consistent. Additional analyses demonstrated the robustness of the D67 to sudden changes in walking speed, limping, changing stride length, and sudden stops or halts of walking. Furthermore, this study tested the D67's performance with an active exoskeleton to determine its reliability in interaction with such a device. Finally the D67 model exhibits comparable or superior performance to the state-of-the-art gait phase estimators.

Our gait phase estimator is designed toward enhancing comfort and performance of exoskeleton-assisted walking for impaired individuals. Collected dateset is, however, obtained from healthy people simulating some pathological gait patterns which does not fully represent the complexity and variability of an impaired gait. Further evaluation is, therefore, required on individuals with impaired gait to further assess the robustness of the proposed method. Inclusion of such pathological walking data in training process as well as implementing our gait phase estimator in different assist-as-needed controllers are considered as the future steps.

References

[1] B. Hobbs and P. Artemiadis, "A review of robot-assisted lower-limb stroke therapy: Unexplored paths and future directions in gait rehabilitation," *Frontiers Neurorobotics*, vol. 14, p. 19, Apr. 2020.

[2] S. A. Murray, K. H. Ha, and M. Goldfarb, "An assistive controller for a lower-limb exoskeleton for rehabilitation after stroke, and preliminary assessment thereof," in *Proc. 36th Annu. Int. Conf. IEEE Eng. Med. Biol. Soc.*, Aug. 2014, pp. 4083–4086.

[3] V. S. Huang and J. W. Krakauer, "Robotic neurorehabilitation: A computational motor learning perspective," *J. Neuroeng. Rehabil.*, vol. 6, no. 5, pp. 1–13, Jan. 2009.

[4] I. Schwartz and Z. Meiner, "Robotic-assisted gait training in neurological patients: Who may benefit?" *Ann. Biomed. Eng.*, vol. 43, no. 5, pp. 1260–1269, 2015.

[5] Y. Ding, A. Kastin, and W. Pan, "Neural plasticity after spinal cord injury," *Current Pharmaceutical Des.*, vol. 11, no. 11, pp. 1441–1450, Apr. 2005.

[6] C. Morawietz and F. Moffat, "Effects of locomotor training after incomplete spinal cord injury: A systematic review," *Arch. Phys. Med. Rehabil.*, vol. 94, no. 11, pp. 2297–2308, 2013.

[7] T. Yan, M. Cempini, C. M. Oddo, and N. Vitiello, "Review of assistive strategies in powered lower-limb orthoses and exoskeletons," *Robot. Auto. Syst.*, vol. 64, pp. 120–136, Feb. 2015.

[8] J. F. Israel, D. D. Campbell, J. H. Kahn, and T. G. Hornby, "Metabolic costs and muscle activity patterns during robotic- and therapist-assisted treadmill walking in individuals with incomplete spinal cord injury," *Phys. Therapy*, vol. 86, no. 11, pp. 1466–1478, 2006.

[9] A. Duschau-Wicke, J. V. Zitzewitz, A. Caprez, L. Lunenburger, and R. Riener, "Path control: A method for patient-cooperative robot-aided gait rehabilitation," *IEEE Trans. Neural Syst. Rehabil. Eng.*, vol. 18, no. 1, pp. 38–48, Feb. 2009.

[10] D. A. Winter, *Biomechanics and Motor Control of Human Movement*. Hoboken, NJ, USA: Wiley, 2009.

[11] H. F. Maqbool, M. A. B. Husman, M. I. Awad, A. Abouhossein, N. Iqbal, and A. A. Dehghani-Sanij, "A real-time gait event detection for lower limb prosthesis control and evaluation," *IEEE Trans. Neural Syst. Rehabil. Eng.*, vol. 25, no. 9, pp. 1500–1509, Sep. 2016.

[12] N. Thatte, T. Shah, and H. Geyer, "Robust and adaptive lower limb prosthesis stance control via extended Kalman filter-based gait phase estimation," *IEEE Robot. Autom. Lett.*, vol. 4, no. 4, pp. 3129–3136, Oct. 2019.

[13] H. Lee, E. J. Rouse, and H. I. Krebs, "Summary of human ankle mechanical impedance during walking," *IEEE J. Transl. Eng. Health Med.*, vol. 4, pp. 1–7, 2016.

[14] A. Arami, E. Van Asseldonk, H. Van Der Kooij, and E. Burdet, "A clustering-based approach to identify joint impedance during walking," *IEEE Trans. Neural Syst. Rehabil. Eng.*, vol. 28, no. 8, pp. 1808–1816, Aug. 2020.

[15] D. A. Winter, "Foot trajectory in human gait: A precise and multifactorial motor control task," *Phys. Therapy*, vol. 72, pp. 45–53, Jan. 1992.

[16] T. Lenzi, M. C. Carrozza, and S. K. Agrawal, "Powered hip exoskeletons can reduce the user's hip and ankle muscle activations during walking," *IEEE Trans. Neural Syst. Rehabil. Eng.*, vol. 21, no. 6, pp. 938–948, Nov. 2013.

[17] C. L. Lewis and D. P. Ferris, "Invariant hip moment pattern while walking with a robotic hip exoskeleton," *J. Biomech.*, vol. 44, no. 5, pp. 789–793, Mar. 2011.

[18] D. Quintero, D. J. Villarreal, D. J. Lambert, S. Kapp, and R. D. Gregg, "Continuous-phase control of a powered knee–ankle prosthesis: Amputee experiments across speeds and inclines," *IEEE Trans. Robot.*, vol. 34, no. 3, pp. 686–701, Jun. 2018.

[19] W. Hong, N. Anil Kumar, and P. Hur, "A phase-shifting based human gait phase estimation for powered transfemoral prostheses," *IEEE Robot. Autom. Lett.*, vol. 6, no. 3, pp. 5113–5120, Jul. 2021.

[20] R. Ronsse *et al.*, "Oscillator-based assistance of cyclical movements: Model-based and model-free approaches," *Med. Biol. Eng. Comput.*, vol. 49, no. 10, pp. 1173–1185, 2011.

[21] T. Yan, A. Parri, V. R. Garate, M. Cempini, R. Ronsse, and N. Vitiello, "An oscillator-based smooth real-time estimate of gait phase for wearable robotics," *Auton. Robots*, vol. 41, no. 3, pp. 759–774, May 2017.

[22] X. Wu, Y. Ma, X. Yong, C. Wang, Y. He, and N. Li, "Locomotion mode identification and gait phase estimation for exoskeletons during continuous multilocomotion tasks," *IEEE Trans. Cognit. Develop. Syst.*, vol. 13, no. 1, pp. 45–56, Mar. 2019.

[23] E. Zheng, S. Manca, T. Yan, A. Parri, N. Vitiello, and Q. Wang, "Gait phase estimation based on noncontact capacitive sensing and adaptive oscillators," *IEEE Trans. Biomed. Eng.*, vol. 64, no. 10, pp. 2419–2430, Oct. 2017.

[24] D. Aoyagi, W. E. Ichinose, S. J. Harkema, D. J. Reinkensmeyer, and J. E. Bobrow, "A robot and control algorithm that can synchronously assist in naturalistic motion during body-weight-supported gait training following neurologic injury," *IEEE Trans. Neural Syst. Rehabil. Eng.*, vol. 15, no. 3, pp. 387–400, Sep. 2007.

[25] I. Kang, P. Kunapuli, and A. J. Young, "Real-time neural network-based gait phase estimation using a robotic hip exoskeleton," *IEEE Trans. Med. Robot. Bionics*, vol. 2, no. 1, pp. 28–37, Feb. 2019.

[26] K. Seo *et al.*, "RNN-based on-line continuous gait phase estimation from shank-mounted IMUs to control ankle exoskeletons," in *Proc. IEEE 16th Int. Conf. Rehabil. Robot. (ICORR)*, Jun. 2019, pp. 809–815.

[27] M. Sarshar, S. Polturi, and L. Schega, "Gait phase estimation by using LSTM in IMU-based gait analysis—Proof of concept," *Sensors*, vol. 21, no. 17, p. 5749, Aug. 2021.

[28] J. Lee, W. Hong, and P. Hur, "Continuous gait phase estimation using LSTM for robotic transfemoral prosthesis across walking speeds," *IEEE Trans. Neural Syst. Rehabil. Eng.*, vol. 29, pp. 1470–1477, 2021.

[29] I. Kang, D. D. Molinaro, S. Duggal, Y. Chen, P. Kunapuli, and A. J. Young, "Real-time gait phase estimation for robotic hip exoskeleton control during multimodal locomotion," *IEEE Robot. Autom. Lett.*, vol. 6, no. 2, pp. 3491–3497, Apr. 2021.

[30] S. P. Nair, S. Gibbs, G. Arnold, R. Abboud, and W. Wang, "A method to calculate the centre of the ankle joint: A comparison with the Vicon® Plug-in-Gait model," *Clin. Biomech.*, vol. 25, no. 6, pp. 582–587, Jul. 2010.

[31] E. B. Titianova, K. Pitkänen, A. Pääkkänen, J. Sivenius, and I. M. Tarkka, "Gait characteristics and functional ambulation profile in patients with chronic unilateral stroke," *Amer. J. Phys. Med. Rehabil.*, vol. 82, no. 10, pp. 778–786, 2003.

[32] K. K. Patterson, W. H. Gage, D. Brooks, S. E. Black, and W. E. McIlroy, "Evaluation of gait symmetry after stroke: A comparison of current methods and recommendations for standardization," *Gait Posture*, vol. 31, no. 2, pp. 241–246, 2010.

[33] H. J. Woltring, "A Fortran package for generalized, cross-validatory spline smoothing and differentiation," *Adv. Eng. Softw.*, vol. 8, no. 2, pp. 104–113, 1986.

[34] C. M. O'Connor, S. K. Thorpe, M. J. O'Malley, and C. L. Vaughan, "Automatic detection of gait events using kinematic data," *Gait Posture*, vol. 25, no. 3, pp. 469–474, Mar. 2007.

[35] A. Waibel, T. Hanazawa, G. Hinton, K. Shikano, and K. J. Lang, "Phoneme recognition using time-delay neural networks," *IEEE Trans. Acoust., Speech, Signal Process.*, vol. 37, no. 3, pp. 328–339, Mar. 1989.

[36] M. F. Møller, "A scaled conjugate gradient algorithm for fast supervised learning," *Neural Netw.*, vol. 6, no. 4, pp. 525–533, Jan. 1993.

[37] C. Lea, M. D. Flynn, R. Vidal, A. Reiter, and G. D. Hager, "Temporal convolutional networks for action segmentation and detection," in *Proc. IEEE Conf. Comput. Vis. Pattern Recognit. (CVPR)*, Jul. 2017, pp. 156–165.

[38] W. Choi, W. Yang, J. Na, G. Lee, and W. Nam, "Feature optimization for gait phase estimation with a genetic algorithm and Bayesian optimization," *Appl. Sci.*, vol. 11, no. 19, p. 8940, Sep. 2021.